ELSEVIER

European Journal of Cardio-thoracic Surgery 29S (2006) S158—S164

EUROPEAN JOURNAL OF CARDIO-THORACIC SURGERY

www.elsevier.com/locate/ejcts

Visualization of tissue velocity data from cardiac wall motion measurements with myocardial fiber tracking: principles and implications for cardiac fiber structures

Bernd André Jung *, Björn W. Kreher, Michael Markl, Jürgen Hennig

Department of Diagnostic Radiology, Medical Physics, Hugstetterstr. 55, D-79106 Freiburg, University of Freiburg, Germany

Received 22 February 2006; accepted 27 February 2006

Abstract

Objective: The spatial arrangement of myocardial fiber structure affects the mechanical and electrical properties of the heart. Therefore, information on the structure and dynamics of the orientation of the muscle fibers in the human heart might provide significant insight into principles of the mechanics of normal ventricular contraction and electrical propagation and may subsequently aid pre- and postsurgical evaluation of patients. Fiber orientation is inherently linked to cardiac wall motion, which can be measured with phase contrast magnetic resonance imaging (MRI), also termed tissue phase mapping (TPM). **Methods:** This study provides initial results of the visualization of velocity data with fiber tracking algorithms and discusses implications for the fiber orientations. In order to generate datasets with sufficient volume coverage and resolution TPM measurements with three-dimensional (3D) velocity encoding were executed during breath-hold periods and free breathing. Subsequent postprocessing evaluation with a tracking algorithm for acceleration fields derived from the velocity data was performed. **Results:** Myocardial acceleration tracking illustrated the dynamics of fiber structure during four different phases of left ventricular performance, that include isovolumetric contraction (IVC), mid-systole, isovolumetric relaxation (IVR), and mid-diastole. Exact reconstruction of the myocardial fiber structure from velocity data requires mathematical modeling of spatiotemporal evolution of the velocity fields. **Conclusions:** 'Acceleration fibers' were reconstructed at these four phases during the cardiac cycle, and these findings may become (a) surrogate parameters in the normal ventricle, (b) baseline markers for subsequent clinical studies of abnormal hearts with altered architecture, and (c) may help to explain and illustrate functional features of cardiac performance in structural models like the helical ventricular myocardial band.

Keywords: Spatial myocardial fiber orientation; Magnetic resonance imaging; Tissue phase mapping; Sequential heart motion; Helical ventricular myocardial band; Acceleration fiber tracking

1. Introduction

The spatial organization of myocardial fiber architecture affects many of the mechanical and electrical properties of the heart, influencing mechanical contraction [1] and electrical propagation [2] in the normal ventricle. Fuller understanding of natural fiber orientation may serve as a baseline for recognizing how alterations in the normal myocardial fiber structure may impact function in diseases that disrupt this normal pattern, such as ischemic heart disease [3] and ventricular hypertrophy [4]. These alterations may predispose the myocardium to abnormal mechanical contraction and electrical propagation [2]. This structure/function interplay is essential for any comprehensive description of the basics of ventricular performance in proposed architectural models, like the helical ventricular myocardial band.

The heart primarily consists of muscle cells, which are bundled together in fibers. These muscle fibers are arranged anisotropically in the heart wall, shown with histologic cross-sections that demonstrate that fibers in subendocardial and subepicardial regions are oriented in opposed directions [5,6]. Subepicardial regions shorten along the direction of the fibers themselves, whereas subendocardial regions exhibit a significant component of shortening perpendicular to the fiber direction (cross-fiber shortening) [7,8]. The impact of the arrangement of the muscle fibers on these different fiber-shortening properties is not fully understood. Based on the helical ventricular myocardial band it is postulated that the arrangement of the muscle fibers are of a great importance for the function of the heart [9,10].

A non-invasive method to determine information on the structure of the muscle fibers in the human heart would therefore be of a great interest for the investigation of the relation between the heart wall motion and the geometry of

* Corresponding author. Tel.: +49 761 270 7393; fax: +49 761 270 3831.
E-mail address: bernd.jung@uniklinik-freiburg.de (B.A. Jung).

1010-7940/$ — see front matter © 2006 Elsevier B.V. All rights reserved.
doi:10.1016/j.ejcts.2006.02.060

the fibers. Information on the interaction of structure and function during the cardiac cycle in the normal heart may become a fundamental concept that underlies medical and surgical interventions aimed at correction of dysfunction produced by diseases, where abnormal cardiac mechanical contraction and electrical propagation is adversely changed.

Previously reported approaches for the extraction of information about the myocardial fiber structure in vivo consist of diffusion magnetic resonance imaging (MRI) using stimulated echoes [11–13]. An intrinsic drawback of these techniques is the use of echo planar imaging for data acquisition. Susceptibility and motion artifacts often provide image quality not sufficient for the clinical routine. Furthermore, diffusion measurements are inherently motion sensitive, and may become adversely affected by breathing- and cardiac motion which is difficult to control due to the extremely high motion sensitivity of such techniques.

Nevertheless, MR imaging provides useful and reliable non-invasive tools for the investigation of myocardial function. Beside a subjective observation of the wall motion with cine imaging techniques, methods for the assessment of regional and global heart wall motion were introduced [14,15]. Established methods to quantify myocardial wall motion include tagging [16], phase contrast velocity mapping (tissue phase mapping, TPM) [17], and displacement encoding with stimulated echoes (DENSE) [18]. Of these, TPM provides high spatial resolution of the functional information (i.e. myocardial motion), which is limited in tagging by the number and density of the grid points. Furthermore, TPM provides time-resolved information compared to DENSE and a higher spatial resolution compared to the recently presented 2D-Cine-DENSE method [19].

To date, no attempts have been reported to derive information about the fiber structures of the ventricles from functional TPM datasets. Since muscle force acts along the fibers, the observed spatiotemporal myocardial velocity over the cardiac cycle is inherently related to the fiber structure. Exact reconstruction of the fiber orientation from functional measurements requires suitable mechanical modeling and knowing how intraventricular blood data influence force vectors in order to solve the inverse problem of extracting the orientation of force vectors (and thus the fibers) from the velocities as a result of these forces. This is beyond the scope of this paper, which describes a first approach using a direct application of tracking algorithms to acceleration vector fields derived from the time-resolved velocity fields of the whole left ventricle (LV) as measured by TPM with velocity encoding in all three dimensions.

2. Theoretical considerations

The motion of the myocardium is a result of the complex spatiotemporal interaction of the force expressed by the myocardial fibers successively triggered by the pathway of electrostimulation. The interaction with blood flowing through the cardiac chambers and the resistance of the ventricular 'hemoskeleton' is governed by the action of the valves and lead to high-pressure phases during valve closure and isobaric phases during blood ejection. The full extend of these interactions is still not fully understood. Exact

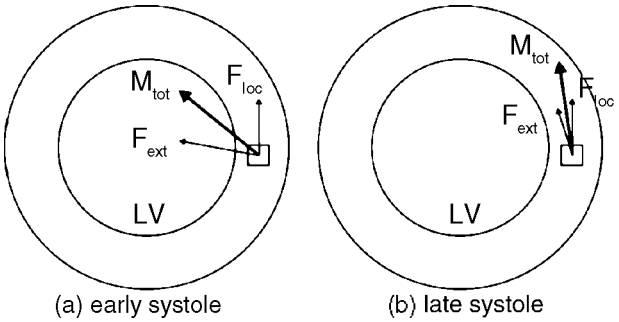

Fig. 1. Schematical representation of the different forces resulting in the observed ventricular wall motion within a pixel. F_{loc} denotes the actual force of the muscle fiber within the pixel, F_{ext} contains external forces caused by other fibers linked by the elasticity of the myocardial tissue and resistive forces from the blood in the heart chamber, and M_{tot} is the momentum acquired as the result of the preceding motion. For example, in early systole F_{loc} and F_{ext} act in different directions (a), in late systole the velocity vectors show their best approximation to the local force vector (b).

reconstruction of fiber orientations from velocity data requires solving the inverse problem of electromechanical modeling including the hemodynamic components and constitutes a considerable task for the future.

The observed ventricular wall motion velocities in each pixel will depend on separate forces: the actual force F_{loc} of the muscle fiber within the pixel, the external force F_{ext}, and the momentum M_{tot} acquired as the result of the preceding motion (see Fig. 1a). F_{ext} contains components from locations along the same fiber, which act in the same direction as F_{loc}, but also resultant forces from all other fibers linked by the elasticity of the myocardial tissue. Additionally, resistive forces from the blood in the heart chamber have to be included. Based on the assumption that accelerations are more related to the development of force than the velocities, a tracking was performed using derived acceleration fields.

Two different kinds of fiber shortenings are described in the literature, one in the longitudinal direction of the fibers and the cross-fiber shortening which seems to be mainly responsible for the thickening of the subendocardial regions of the heart [7]. The anatomical fiber structure is described by tangential components only, whereas geometrical contraction also contains the cross-fiber terms for the wall thickening. For a better description of the fiber component, one can thus assume that all velocity components in the radial direction are caused by external forces F_{ext}. Velocity component perpendicular to the endocardial wall are therefore discarded.

However, there are four classical phases within the cardiac cycle that include isovolumetric contraction (IVC, before the aortic valve opens), ventricular ejection during mid-systole, isovolumetric relaxation (IVR) after ejection during early diastole, after which rapid ventricular filling occurs, and finally the diastolic interval where passive ventricular filling. These four time intervals are associated with the four cardiac motions of narrowing, shortening, lengthening, and widening. Of great interest, a sequence of clockwise and counterclockwise motions exists with variances between the basal and apical segments with a reciprocal twist of the heart as it undergoes through these phases of isovolumetric contraction, ejection, rapid filling and passive filling during diastole.

The purpose of this report is to link these motions to changes in fiber orientation suggested by the foregoing analysis of acceleration vector fields derived from the time-resolved velocity fields. This intervention may provide an early insight into how suggested spatial anatomic fiber orientation pathways derived from the helical ventricular myocardial band interact with non-invasive functional measurements made by TPM.

3. Materials and methods

3.1. Data acquisition

All experiments were performed on a Siemens Sonata 1.5 T scanner (Siemens Medical Solutions, Erlangen, Germany). All measurements were performed with a four-element-phased array body coil on healthy volunteers. Human studies were approved by the local ethics committee and informed consent was obtained from all subjects.

TPM images were acquired with a gradient echo sequence as described previously [20,21] with a spatial resolution of 1.3 mm $\times$ 1.3 mm. Data were acquired in two volunteers with a breath-hold sequence and a respiratory-gated free-breathing sequence both with a temporal resolution of 64 ms. The full velocity information of the beating heart was obtained in 25 heartbeats within a single breath-hold measurement. Furthermore, a dataset was acquired with a respiratory-gated free-breathing measurement [22] with the same spatial but a higher temporal resolution of 13.8 ms. The whole LV was covered with nine gapless short-axis slices of 8 mm thickness from base to apex.

3.2. Postprocessing

Data postprocessing was performed on a personal computer using customized software programmed in Matlab (The Mathworks). After contour segmentation and a correction for translational motion components of the LV [20], the resulting velocity vector was calculated from the measured *x*-, *y*-, and *z*-velocity components. Subsequently, pixelwise myocardial acceleration vectors were calculated from the time-resolved velocity data by calculating discrete temporal derivatives. Tracking of acceleration fields was performed based on fiber tracking algorithms for diffusion tensor imaging of the brain [23] as proposed by Mori et al. [24]. In this implementation, two criteria define the existence of tracks. A track was terminated if the maximum angle deviation of the acceleration vectors between adjacent voxels exceeded 30°. In addition, a minimum length of 10 voxels along the track was required. The exclusion of the motion component normal to the ventricular wall (i.e. radial motion component) was performed by a projection of the velocity vector of each voxel onto the corresponding tangential wall segment which was calculated from the three dimensional (3D) segmentation mask. For tracking, data was interpolated in the long-axis direction to a doubled number of slices in this direction due to the low spatial resolution (8 mm slice thickness). The global track angle with respect to the circumferential plane (see Fig. 4, left) for all identified tracks in each slice was calculated. The tracking algorithm was applied for four different time frames within the cardiac cycle: (a) IVC, (b) mid-systole, (c) IVR, and (d) mid-diastole.

4. Results

MR imaging permits the measurement of different LV motion components involving a complex interaction of contraction, shortening and twisting as known from echocardiography. To illustrate the nature of such TPM raw data used for calculation of acceleration fields, tracking and identification of characteristic time frames, Fig. 2 shows pixelwise arrow plots of the in-plane velocity component in the short-axis view of the four above-mentioned cardiac frames. Hereby, the large arrows represent the mean velocities in eight left ventricular angular areas of equal size for better visualization. Initially measured cartesian velocity components were transformed into radial and tangential velocities, representing the myocardial motion in the short-axis view in terms contraction/expansion (radial velocities) and clockwise/counterclockwise rotation (tangential velocities). Shortening and lengthening of the LV is governed by the additionally measured longitudinal velocity component. The dominant motional behavior (i.e. average over the entire basal slice) is shown in the time courses of global radial (e), tangential (f), and longitudinal (g) velocities over the cardiac cycle. The temporal locations within the RR-interval of the four arrow plots (top row) are indicated by the small circles in these graphs. The same time frames were used for the tracking of the derived acceleration fields.

Based on TPM raw data shown in Fig. 2, acceleration tracks were calculated representing the local acceleration field potentially linked to forces acting along the direction of fibers and thus fiber orientation. Fig. 3 shows a projection on a long axis of the LV of all identified tracks with a breath-hold dataset (a) and a free-breathing dataset (b) demonstrating the mismatch between adjacent slices (left) during breath-hold periods. In contrast, free-breathing measurements (right) result in smoother tracks and improved coverage of the LV.

In order to illustrate temporal changes in track orientation, Fig. 4 shows a three-dimensional depiction of the identified acceleration tracks for four different cardiac frames. The tracks show a smooth and helical coverage of the entire LV for the cardiac frame during IVC (a) representing the onset of shortening and counterclockwise rotation (viewed from apex to base) of the entire LV. Compared to IVC, simultaneous changes in longitudinal (deceleration) and rotational (change of direction) motion in mid-systole, result in similar helicity with a somewhat decreased track angle. During IVR, a different tilt of the identified tracks in base and apex (c) can be identified indicating initial lengthening and more complex rotational behavior. While apical regions demonstrate considerable change in rotation, basal slices are dominated by lengthening and exhibit only minor twisting. In mid-diastole, myocardial action is mostly governed by a change of the longitudinal motion component (lengthening) only (d).

In general, due to the complex rotational motion behavior of the LV (see also Fig. 2f) the tracks change their orientation

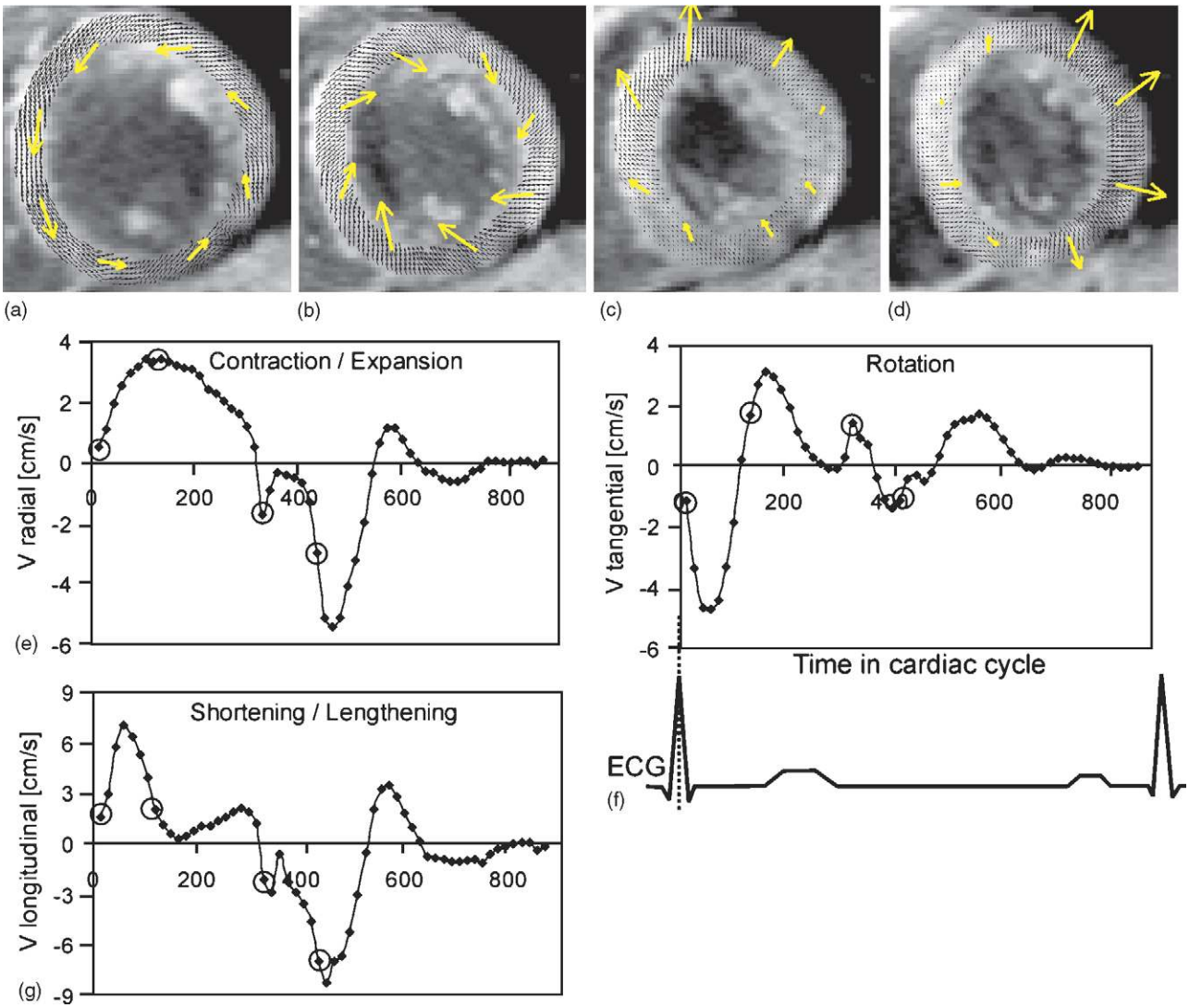

Fig. 2. Top: pixelwise arrow plots of the in-plane velocity component in a basal short-axis view for a healthy volunteer: cardiac frames during (a) IVC, (b) mid-systole, (c) IVR, and (d) mid-diastole. The large arrows represent the mean velocities in eight left ventricular angular areas of equal size for better visualization. Bottom: global radial, tangential and longitudinal velocities illustrating the dominant motional behavior over the cardiac cycle. The small circles indicate the temporal location of the arrow plots within the cardiac cycle.

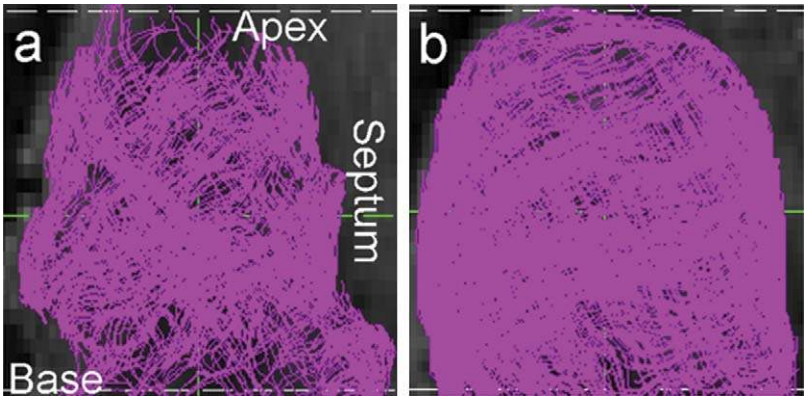

Fig. 3. Projection of all identified tracks in a long-axis view of the left ventricle with a breath-hold dataset (a) and a free-breathing dataset (b) demonstrating the mismatch between adjacent slices during breath-hold periods.

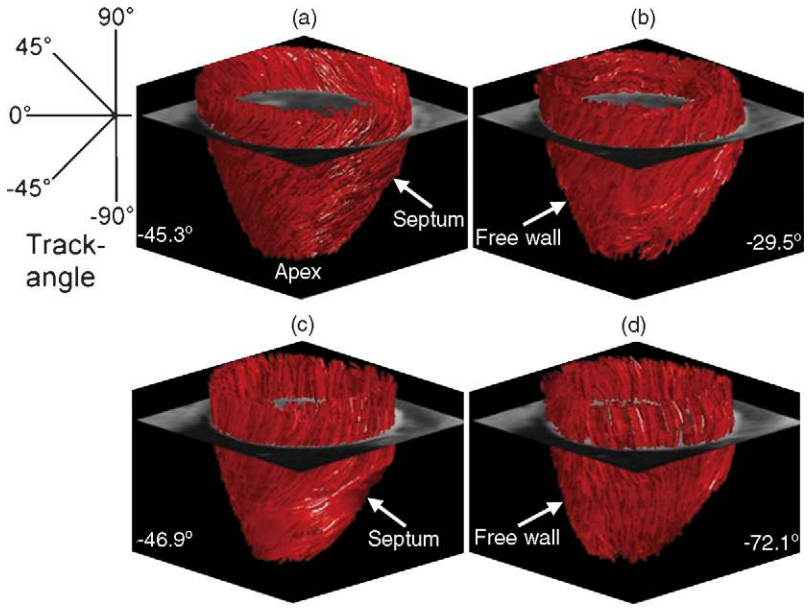

Fig. 4. 3D-depiction of the identified acceleration tracks: cardiac frames during (a) IVC, (b) mid-systole, (c) IVR, and (d) mid-diastole. The definition of the track angle orientation is shown on the left side. The global track angle over the entire LV is given in each depicted cardiac frame.

dependent on the time point during the cardiac cycle. Track angles therefore permit the quantitative description of local and global track orientation. The definition for the track angle orientation is shown in the schematic diagram on the left side (see also Fig. 5). The mean angle of all identified acceleration tracks is given in the corner for the depicted cardiac frames. For illustration purposes only about 25% (~2500) of all randomly chosen identified tracks are depicted.

To illustrate the local dependence of track angle orientation on long-axis location, Fig. 5 shows the mean angles of the identified acceleration tracks in individual circumferential (short axis) planes from apex to base for the same four cardiac frames as shown in Fig. 4: IVC, mid-systole, IVR, and mid-diastole. Consistent with the 3D-visualization of tracks in Fig. 4c, considerable variation of mean track angle from base to apex can be clearly identified for IVR.

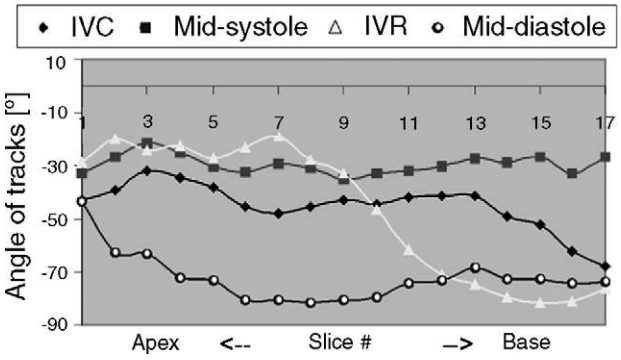

Fig. 5. Global angle with respect to the short-axis plane of the identified acceleration tracks over all slices from apex to base: cardiac frames during IVC (diamond), mid-systole (gray square), IVR (white triangle), and mid-diastole (black/white circle).

5. Discussion

In order to investigate if relevant information characterizing myocardial fiber architecture could be extracted from functional MRI data, the novel idea of a tracking of acceleration fields of the left ventricle based on TPM data was presented.

The parameterized data were improved by the use of a respiratory-gated free-breathing acquisition strategy and by track calculation without the motion component perpendicular to the myocardial wall leading to better coverage by the identified tracks. Results for measurements with free breathing compared to sequential breath-hold acquisition demonstrate consistent high quality of the respiratory gating approach, whereas breath-hold images suffer from data inconsistency due to imperfect repositioning between breath-holds. In terms of image processing the algorithms used are commonly applied to generate streamlines in fluid studies. Since the term 'streamlines' implies transportation processes, which is clearly not applicable to tissue velocity data, the more appropriate term 'tracks' was used in this work.

As shown in Fig. 4, it can be qualitatively visualized that the inclination of the tracks with respect to the circumferential plane changes in different cardiac frame and inside a cardiac frame dependent from the location (e.g. Fig. 4c). Although the tracks show an identical helicity in, for example, (a) and (c), the acceleration vectors show in opposite directions since the longitudinal and the rotational motion components have both different signs in (a) and (c) (see time courses in Fig. 2).

If the action exerted by the myocardial fibers themselves (F_{loc}) is the dominant force, the measured velocity will be in good approximation point along the direction of the fibers and velocity vectors can be used to directly detect fiber orientation. However, this condition is never strictly met, but

it is possible to use derived acceleration fields to improve the approximation to the local fiber force vector. Generally, tracking results may improve if fibers will have acted approximately coherently in the same overall direction before velocity changes as a result of altering forces occur (e.g. during mid-systole, see also Fig. 1). Although the measured velocity direction can be expected to somewhat deviate from the structural fiber orientation, it may be hypothesized that this is at least consistently related to structural fiber orientation. For interindividual comparison, it can thus be assumed that a more inclined acceleration vector with respect to the circumferential plane indicates a more diagonal arrangement of the fiber structure at equivalent time points in the ECG-cycle. Based on the hypothesis that a more diagonal arrangement of muscle fibers leads to a more efficient cardiac output, the track angle with respect to the circumferential plane could be an interesting parameter to investigate. Fig. 5 shows that the angle of the acceleration track can change dependent from the region in the LV (e.g. lower track angles near the apex and higher track angles towards the base for cardiac frame during IVR).

Note that the identified tracks do not necessarily correspond to the direction of existing anatomical muscle fibers. This is due to the complex motion of the heart wall which is characterized by an interaction between the local instant force and global forces such as the momentum of inertia. The aim of this heuristic parametrization is not primarily an exact biometric characterization of the structural fiber orientation, but rather the determination of surrogate parameters that are stable and reproducible. Such parameters might be useful for the characterization of the motion geometry during therapy treatment for the individual patient as well as for the diagnosis in the interindividual comparison.

An assessment of the extend to which the generated velocity fibers conform with the structural fiber orientation requires a comparison of our velocity-based evaluation with postmortem structural evaluation. For humans, such a comparison is clearly impossible, and hopefully large or small animal studies may be developed for demonstration of a biometric correspondence. The ratio of the pertinent forces F_{loc}, F_{ext}, and M_{tot} can, however, not be expected to scale linearly with size and such a verification would thus have limited impact on human values. Verification by postmortem evaluation is possible but has to wait until such data can be acquired as a supplement to a study requiring the sacrifice of animals, which will be conducted in the future.

A fundamental limitation of deriving structural fiber information from dynamic velocity data is related to the fact that only net effects within each voxel are observed. For interwoven fiber pathways of different orientations, even sophisticated dynamic modeling can only detect the direction of the resultant force and will thus be unable to identify such criss-cross tissue types. The main purpose of our approach is not the exact assessment of the structural biomechanics, but to derive clinically useful surrogate parameters for further use in patient studies. In a first step, the biometric verification appears to be of secondary importance. For that, the primary aim will be to assess, whether derived surrogate parameters (fiber orientation, fiber length . . .) provide useful parameters for clinical studies and/or improved understanding of ventricular performance. Further volunteer and patient investigations are necessary to perform a detailed analysis of the derived tracking data. In addition, a more detailed evaluation of different cardiac phases could provide more information on subregions of the ventricular wall and may resolve contributions of different muscle layers to the heart wall motion. This may help to elucidate and distinguish different models of cardiac structure such as the helical ventricular myocardial band.

This concept of a resultant force is implied by prior ultrasonic crystal measurements [25], whereby the crystals were placed into the angulation of the presumed functional units of the descending and ascending segments of the apical loop of the helical ventricular myocardial band. It would be of great interest for future studies to compare the direction of maximum shortening of ultrasonic crystal pairs with tracking results of velocity and acceleration fields obtained by TPM measurements.

For a better understanding of the function of the heart muscle, electro-mechanical heart models have been developed, which consider the electro-physiology of the cells, the electrical propagation in tissue and, the elasto-mechanical properties of the heart [26]. Different heart models have been presented including continuum-mechanical models [27], and discrete models that base on a spring-mass system [28]. These heart models simulate the cardiac wall motion considering the electrical propagation and the anisotropic mechanical properties of tissue, the viscosity of blood, and particularly the orientation of the myocardial fiber structure [29]. The application of such an electro-mechanical heart model to the motion describing TPM data could be used to verify the plausibility of the presented data-driven evaluation. Based on such a model, a calculation using simulated ideal fiber distribution could potentially determine if and how far the calculated motion pattern reflects the above hypothesis. In reverse, the model could be used to investigate if the motion describing vectors calculated with the velocity or acceleration tracks agree with the measured data.

6. Conclusion

In conclusion, a novel method for the tracking of velocity and acceleration fields of the left ventricle based on tissue phase mapping data was presented. New information is provided by the calculated velocity and acceleration tracks. Data acquisition was improved by the use of a respiratory-gated free-breathing acquisition strategy.

References

[1] Waldman LK, Nosan D, Villarreal F, Covell JW. Relation between transmural deformation and local myofiber direction in canine left ventricle. Circ Res 1988;63(3):550—62.
[2] Chen PS, Cha YM, Peters BB, Chen LS. Effects of myocardial fiber orientation on the electrical induction of ventricular fibrillation. Am J Physiol 1993;264(6 Pt 2):H160—73.
[3] Wickline SA, Verdonk ED, Wong AK, Shepard RK, Miller JG. Structural remodeling of human myocardial tissue after infarction. Quantification with ultrasonic backscatter. Circulation 1992;85(1):259—68.

[4] Koide T, Narita T, Sumino S. Hypertrophic cardiomyopathy without asymmetric hypertrophy. Br Heart J 1982;47(5):507—10.
[5] Fox CC, Hutchins GM. The architecture of the human ventricular myocardium. Johns Hopkins Med J 1972;130(5):289—99.
[6] Greenbaum RA, Ho SY, Gibson DG, Becker AE, Anderson RH. Left ventricular fibre architecture in man. Br Heart J 1981;45(3):248—63.
[7] Rademakers FE, Rogers WJ, Guier WH, Hutchins GM, Siu CO, Weisfeldt ML, Weiss JL, Shapiro EP. Relation of regional cross-fiber shortening to wall thickening in the intact heart. Three-dimensional strain analysis by NMR tagging. Circulation 1994;89(3):1174—82.
[8] MacGowan GA, Shapiro EP, Azhari H, Siu CO, Hees PS, Hutchins GM, Weiss JL, Rademakers FE. Noninvasive measurement of shortening in the fiber and cross-fiber directions in the normal human left ventricle and in idiopathic dilated cardiomyopathy. Circulation 1997;96(2):535—41.
[9] Buckberg GS. Seminars in thoracic and cardiovascular surgery. Am Assoc Thorac Surg 2001;13:298—416.
[10] Torrent-Guasp F, Kocica MJ, Corno A, Komeda M, Cox J, Flotats A, Ballester-Rodes M, Carreras-Costa F. Systolic ventricular filling. Eur J Cardiothorac Surg 2004;25(3):376—86.
[11] Edelman RR, Gaa J, Wedeen VJ, Loh E, Hare JM, Prasad P, Li W. In vivo measurement of water diffusion in the human heart. Magn Reson Med 1994;32(3):423—8.
[12] Reese TG, Weisskoff RM, Smith RN, Rosen BR, Dinsmore RE, Wedeen VJ. Imaging myocardial fiber architecture in vivo with magnetic resonance. Magn Reson Med 1995;34(6):786—91.
[13] Dou J, Reese TG, Tseng WY, Wedeen VJ. Cardiac diffusion MRI without motion effects. Magn Reson Med 2002;48(1):105—14.
[14] McVeigh ER. MRI of myocardial function: motion tracking techniques. Magn Reson Imaging 1996;14(2):137—50.
[15] Masood S, Yang GZ, Pennell DJ, Firmin DN. Investigating intrinsic myocardial mechanics: the role of MR tagging, velocity phase mapping, and diffusion imaging. J Magn Reson Imaging 2000;12(6):873—83.
[16] Zerhouni EA, Parish DM, Rogers WJ, Yang A, Shapiro EP. Human heart: tagging with MR imaging—a method for noninvasive assessment of myocardial motion. Radiology 1988;169(1):59—63.
[17] Pelc LR, Sayre J, Yun K, Castro LJ, Herfkens RJ, Miller DC, Pelc NJ. Evaluation of myocardial motion tracking with cine-phase contrast magnetic resonance imaging. Invest Radiol 1994;29(12):1038—42.
[18] Aletras AH, Ding S, Balaban RS, Wen H. DENSE: displacement encoding with stimulated echoes in cardiac functional MRI. J Magn Reson 1999;137(1):247—52.
[19] Kim D, Gilson WD, Kramer CM, Epstein FH. Myocardial tissue tracking with two-dimensional cine displacement-encoded MR imaging: development and initial evaluation. Radiology 2004;230(3):862—71.
[20] Hennig J, Schneider B, Peschl S, Markl M, Krause T, Laubenberger J. Analysis of myocardial motion based on velocity measurements with a black blood prepared segmented gradient-echo sequence: methodology and applications to normal volunteers and patients. J Magn Reson Imaging 1998;8(4):868—77.
[21] Markl M, Schneider B, Hennig J. Fast phase contrast cardiac magnetic resonance imaging: improved assessment and analysis of left ventricular wall motion. J Magn Reson Imaging 2002;15(6):642—53.
[22] Jung B, Zaitsev M, Hennig J, Markl M. Navigator gated high temporal resolution tissue phase mapping of myocardial motion. Magn Reson Med 2006, in press.
[23] Basser PJ, Mattiello J, LeBihan D. Estimation of the effective self-diffusion tensor from the NMR spin echo. J Magn Reson B 1994;103(3):247—54.
[24] Mori S, Crain BJ, Chacko VP, van Zijl PC. Three-dimensional tracking of axonal projections in the brain by magnetic resonance imaging. Ann Neurol 1999;45(2):265—9.
[25] Castella M, Buckberg GD, Saleh S, Gharib M. Structure function interface with sequential shortening of basal and apical components of the myocardial band. Eur J Cardiothorac Surg 2005;27(6):980—7.
[26] Hunter PJ, Pullan AJ, Smaill BH. Modeling total heart function. Annu Rev Biomed Eng 2003;5:147—77.
[27] Hunter PJ, McCulloch AD, ter Keurs HE. Modelling the mechanical properties of cardiac muscle. Prog Biophys Mol Biol 1998;69(2/3):289—331.
[28] Mohr MB, Blumcke LG, Sachse FB, Seemann G, Werner CD, Dossel O. Volume-based modeling of deformation in myocardium based on models of force development. Biomed Tech 2002;47:225—8.
[29] Ackerman MJ. The Visible Human Project. J Biocommun 1991;18(2):14.